Energy & Environmental Science

Accepted Manuscript

ROYAL SOCIETY OF CHEMISTRY

www.rsc.org/ees

Journal Name

RSCPublishing

ARTICLE

A single atom change "switches-on" solar-to-energy conversion efficiency on Zn-porphyrin based Dye Sensitized Solar Cell to 10.5%.

Cite this: DOI: 10.1039/x0xx00000x

Received 00th January 2012,
Accepted 00th January 2012

DOI: 10.1039/x0xx00000x

www.rsc.org/

Lydia Cabau,[a] Challuri Vijay Kumar,[a] Antonio Moncho,[a] John N. Clifford,[a] Núria López[a] and Emilio Palomares[a,b*]

In this work we report how crucial is the correct design of the porphyrin sensitizers in Dye Sensitized Solar Cells (DSSC). Only a single atom change *switches-on* the efficiency from 2-3% to efficiencies over 10% under standard measurement conditions. We have used the 2,1,3-benzothiadazole (BDT) group, as a π-conjugated linker, for the porphyrin **LCVC01** a thiophene moiety for the porphyrin **LCVC02** and also the furan group for the **LCVC03** porphyrin, as molecular, spacers between the BDT moiety and the molecule anchoring group, respectively. These three porphyrins were investigated for their application in DSSC devices. The devices were characterized achieving a record cell of 10.5% for **LCVC02** but only a 3.84% and 2.55% were achieved for **LCVC01** and **LCVC03** respectively. In one hand, the introduction of a thiophene, instead of a furan group illustrates the importance to introduce a chemical group as spacer, such as thiophene, between of the BDT and the anchoring group. On the other hand, the election of this group has to be correct because the change of a single atom increases the charge recombination rate and decreases the device performance. These changes can be rationalized by analyzing the dye dipoles and their interactions.

1. Introduction

Dye Sensitized Solar Cells (DSSC) based on mesoporous TiO_2 thin film and liquid electrolytes have already achieved solar-to-energy conversion efficiencies close to 13%[1], a value, which is beyond the current state-of-the art of organic solar cells (OSC) and close to the efficiencies reported for methyl-ammonium lead iodide perovskite based solar cells (MAPI) measured in forward bias[†] (from short circuit, Isc, to open circuit voltage, Voc).

However, the use of liquid based red/ox electrolytes such as iodine/iodide or Cobalt (II)/Cobalt (III) has hampered their progress as a PV (photovoltaic) technology. Nonetheless, a recent application of these solar cells in the façade of a building has illustrated its real potential as a robust, colourful and transparent technology for solar-to-energy conversion[††].

Yet, there are several scientific issues that must be investigated further to achieve higher efficiencies by reducing the device losses, that limit the voltage in the DSSC, and approach the maximum theoretical efficiency that is close to 20%[2]. As shown in **Figure 1**, porphyrins based DSSC are capable to reach high photocurrents but Voc is low compared, for example, with OSC and MAPI solar cells.

In 2010, a landmark paper by Yeh and collaborators described the synthesis of so called "push-pull approach" Zn-porphyrins that lead to a remarkable increase in the solar-to-electrical conversion efficiency in porphyrins based DSSC from 5-6% to 11%[3]. Later, this efficiency was increased by using a more sophisticated molecular design of the porphyrin structure and a world-record efficiency of 12.3%[4] was obtained. Since then, the synthesis and use of asymmetric porphyrins has increased exponentially[5] but little attention has been paid to the device function–porphyrin structure relationship through the detailed analysis of the interfacial charge recombination reactions[5d,6] or the porphyrin structure. Indeed, it has been more difficult to understand what are the reasons for which subtle modifications on the porphyrin structure led to substantially decrease in the Voc and, hence, in the cell efficiency under operation conditions and, thus, not many examples of Zn-based porphyrin can be found in the scientific literature that overpass the 10% efficiency value.

Herein, we have focussed, not only on the design of a push-pull porphyrin for efficient DSSC but also on the integral evaluation of the reactions that limit the device Voc, and thus, the efficiency.

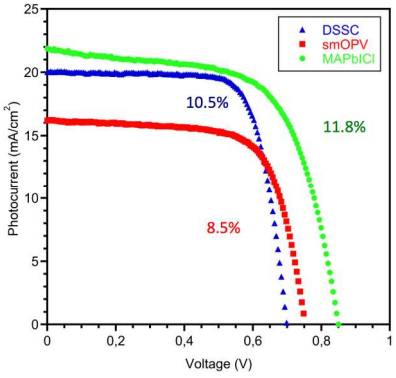

Figure 1. IV curves at 1 sun-simulated 1.5AM G conditions for a LCVC02 porphyrin DSSC (this work) in blue triangles, a MAPI solar cell (green dots) and a OSC based small molecule DR3TBDT: $PC_{70}BM$ (red squares). All devices made at ICIQ.

Figure 2 illustrates the three porphyrins synthetized in this work and used to prepare DSSC.

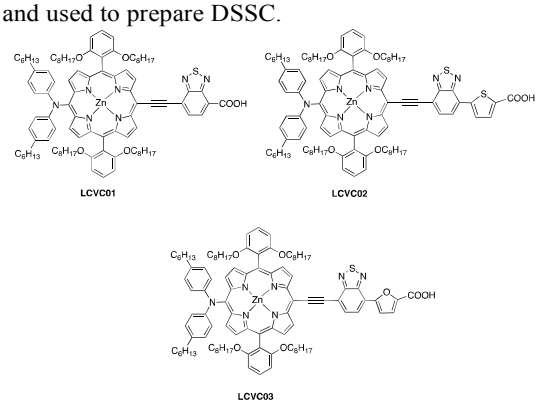

Figure 2 . The molecular structure of porphyrins in LCVC01, LCVC02 and LCVC03 dyes.

2. Experimental Section

2.1.Materials

N,N-Dimethylformamide (DMF) and THF were distilled before use. $Pd^{II}(dppf)Cl_2$, N-bromosuccinimide (NBS), potassium carbonate, 4-tert-butylpyridine (TBP), (5-formylthiophen-2-yl) boronic acid, (5-formylfuran-2-yl) boronic acid, TBAF, $Pd_2(dba)_3$ and $AsPh_3$ were purchased from Sigma-Aldrich.

2.2.Instruments

The UV-Visible absorption was measured using a $1cm^2$ path-length quartz cell on a Shimadzu© UV 1700 spectrophotometer. The steady state fluorescence spectra were carried out using a Spex model Fluoromax-3 spectro-fluorometer using a $1cm^2$ quartz square. The ^{1}H-NMR spectra were measured at 300 MHZ on a Bruker 300 Avance NMR spectrometer with X-Win NMR software. The ^{1}H spectra were referenced to tetramethylsilane. The ESI-MS (Electro Spray Ionisation Mass Spectra) were recorded on a Water Quattro micro (Water, Inc, USA). The cyclic voltammetry experiments were recorded with a PC-controlled CH instruments© model CHI620C electrochemical analyser.

Laser Transient Absorption Spectroscopy (L-TAS), charge extraction (CE) and transient photovoltage (TPV) were carried out as detailed previously[7].

2.3. Synthesis and characterization

The porphyrin intermediate to synthesize **LCVC01**, **LCVC02** and **LCVC03** was synthesized according to the literature[4], Scheme 1.

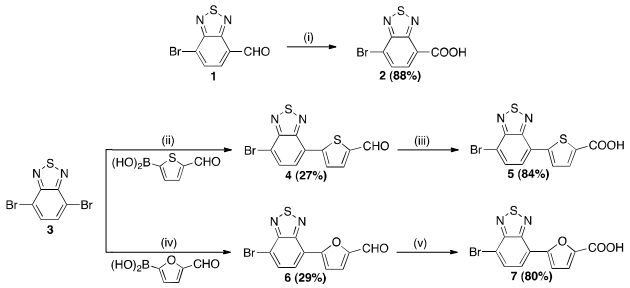

Scheme 1: The synthetic route for the acceptor moieties. (Reaction conditions: (i) $NaClO_2$, sulfamic acid aqueous, acetone, 4 h, RT; (ii) PdII(dppf)Cl_2, 2M K_2CO_3 aqueous solution,THF, 2 h, 76ºC; (iii) $NaClO_2$, sulfamic acid aqueous, acetone, 4 h, RT; (iv) PdII(dppf)Cl2, 2M K2CO3 aqueous solution,THF, 2 h, 76ºC; (v) NaClO2, sulfamic acid aqueous, acetone, 4 h, RT (room temperature).

Synthesis of 7-bromobenzo[*c*][1,2,5]thiadiazole-4-carboxylic acid 2: A solution at 0ºC of 7-bromobenzo[*c*][1,2,5]thiadiazole-4-carbaldehyde (0.1g; 0.41mmol) in acetone (70mL), $NaClO_2$ (0.109g, 1.21mmol), was added slowly. Then, a solution of sulfamic acid (0.117g; 1.21mmol) in Milli-Q-grade deionized water (8mL) was added and the solution was stirred at room temperature for 4h. After, the reaction was quenched with HCl (0.1M, 250mL) and the mixture was extracted with $CHCl_3$. The combined extracts were washed with water and dried over anhydrous $MgSO_4$. The solvent was removed under reduced pressure to give the desired product (white solid). (0.093g, 88% Yield). ^{1}H NMR ($CDCl_3$, 400 MHZ) δ_H: 8.45 (d, J=7.7Hz, 1H); 8.05 (d, J=7.7Hz, 1H).

Synthesis of 5-(7-bromobenzo[*c*][1,2,5]thiadiazol-4-yl)thiophene-2-carbaldehyde (4): In a Schlenk flask, **3** (0.5 g. 1.70mmol), (5-formylthiophen-2-yl) boronic acid (0.268 g, 1.70mmol), $Pd^{II}(dppf)Cl_2$ (0.056 g, 0.0765mmol) and 50ml of THF were added together and the mixture was degassed. Then the solution was stirred at room temperature for 30 minutes. After this period 7 mL of K_2CO_3 2M was added and the mixture was degassed again. Thereafter, the mixture was heated up to 76ºC for 2 hours, cooled at room temperature and extracted with Et_2O, upon adding water, and washed with brine. Finally, the crude was purified by column chromatography using hexane/ethyl Acetate (v:v8:2) as a solvent to give us the desired product (yellow solid) (150mg, 27% Yield). ^{1}H NMR ($CDCl_3$ 400 MHZ) δ_H: 9.95 (s, 1H); 8.25 (d, J=4.0Hz, 1H); 8.06 (d, J=7.7Hz, 1H); 8.00 (dd, J=7.7Hz, 21.0Hz 2H); 7.93 (d, J=4.0Hz, 1H). ^{13}C NMR (100MHz, THF_{d-8}, ppm) δ.□□□□□□□□ 162.87; 160.35; 153.92; 145.65; 136.99; 134.36; 132.99; 129.00; 128.05; 115.27□ MS-ESI (*m/z*): [M-H] calculated for $C_{11}H_4N_2BrN_2OS_2$: 322.8954; found: 322.8958. (^{1}H-NMR and HRMS(ESI) spectra are shown in the supporting Information)

Synthesis of 5-(7-bromobenzo[*c*][1,2,5]thiadiazol-4-yl)thiophene-2-carboxylic acid (5): $NaClO_2$ (0.124g, 1,38mmol), was added slowly to at 0ºC solution of 5-(7-bromobenzo[*c*][1,2,5]thiadiazol-4-yl)thiophene-2-carbaldehyde, **4** (150mg; 0.46mmol) in acetone (100mL). Then, a solution of sulfamic acid (0.134g; 1.38mmol) in Milli-Q-grade deionized water (10mL) was added to proceed at room

temperature for 4h. After, the reaction was quenched with HCl (0.1M, 250mL) and the mixture was extracted with $CHCl_3$. The combined extracts were washed with water and dried over anhydrous $MgSO_4$. The solvent was removed under reduced pressure to give as the desired product (white solid). (0.131g, 84% Yield). ^{1}H NMR (DMSO-$_{d6}$, 400 MHZ) δ_H: 8.12 (m, 3H); 7.82 (d, J=4.0Hz, 1H). ^{13}C NMR (100MHz, DMSO-d6, ppm) δ 162.85; 152.94; 150.82; 143.52; 135.81; 133.44; 132.49; 127.95; 127.18; 125.07; 113.22. MS-ESI (*m/z*): [M-H] calculated for $C_{11}H_4N_2BrN_2O_2S_2$: 338.8898; found: 338.8903. (^{1}H-NMR/^{13}C-NMR and HRMS(ESI) spectra are shown in the supporting Information)

Synthesis of 5-(7-bromobenzo[*c*][1,2,5]thiadiazol-4-yl)furan-2-carbaldehyde (6): In a Schlenk flask **3** (0.5 g. 1.70 mmol), (5-formylfuran-2-yl) boronic acid (0.237 g, 1.70mmol), Pd^{II}(dppf)Cl_2 (0.056 g, 0.0765mmol) and 50ml of THF was added and the mixture was degassed. Following the degasification, the solution was stirred at room temperature for 30 minutes. Thereafter, 7mL of K_2CO_3 2M were added and the mixture was degassed again. Then the mixture was heated up to 76°C for 2 hours. After cooling at room temperature we added water and the solution was extracted with Et_2O and washed with brine. Then the crude was purified by column chromatography using Hexane/DCM (v:v 8:2) as a solvent to give us the desired product (yellow solid) (0.160g, 29% Yield). ^{1}H NMR ($CDCl_3$, 400 MHZ) δ_H: 9.72(s, 1H); 8.14 (d, J=7.7Hz, 1H); 7.94 (d, J=7.7Hz, 1H); 7.87 (d, J=3.6Hz, 1H); 7.41 (d, J=3.6Hz, 1H); ^{13}C NMR (100MHz, $CDCl_3$, ppm) δ 177.71; 154.39; 154.017; 152.31; 150.92; 132.45; 126.50; 123.88; 121.50; 115.65; 114.89 MS-ESI (*m/z*): $[M+Na]^+$ calculated for $C_{11}H_5N_2BrN_2NaO_2S$: 330.9147; found: 330.9137. (^{1}H-NMR/^{13}C-NMR and HRMS(ESI) spectra are shown in the supporting Information)

Synthesis of 5-(7-bromobenzo[*c*][1,2,5]thiadiazol-4-yl)furan-2-carboxylic acid (7): A solution at 0ºc of 5-(7-bromobenzo[*c*][1,2,5]thiadiazol-4-yl)furan-2-carbaldehyde **6** (0.160 g; 0.51mmol) in acetone (110mL), $NaClO_2$ (0.140 g, 1,55mmol), was added slowly. Then, a solution of sulfamic acid (0.151 g; 1.55mmol) in Milli-Q-grade deionized water (10mL) was added and the solution was then stirred at room temperature for 4h. After the 4 hours, the reaction was quenched with HCl (0.1M, 250mL) and the mixture was extracted with $CHCl_3$. The combined extracts were washed with water and dried over anhydrous $MgSO_4$. The solvent was removed under reduced pressure to give as the desired product (yellow solid). (0.133 g, 80% Yield). ^{1}H NMR (DMSO-$_{d6}$ 400 MHZ) δ_H: 8.12 (d, J=7.7Hz, 1H); 7.99 (d, J=7.7Hz, 1H); 7.69 (d, J=3.6Hz, 1H); 7.42 (d, J=3.6Hz, 1H); ^{13}C NMR (100MHz, DMSO-d6, ppm) δ 159.13; 153.00; 151.44; 149.83; 144.88; 132.54; 125.28; 120.91; 119.82; 113.90; 113.45. MS-ESI (*m/z*): [M-H] calculated for $C_{11}H_4N_2BrN_2O_3S$: 322.9126; found: 322.9137. (^{1}H-NMR/^{13}C-NMR and HRMS(ESI) spectra are shown in the supporting Information)

Synthesis of LCVC01: To a solution of [5-Bis(4-hexylphenyl)amino-15-(Triisopropylsily)ethynyl-10,20-bis(2,6-di-octooxyphenyl)porphirinato] Zinc(II) **8** (240mg, 0.154mmol) in dry THF (20mL) we added TBAF (0.78mL) 1M in THF. The solution was stirred at 23ºC for 30min under N_2. The mixture was quenched with H_2O and then extracted with CH_2Cl_2. The organic layer was dried using anhydrous $MgSO_4$ and the solvent was removed under reduced pressure. The residue and the 7-bromobenzo[*c*][1,2,5]thiadiazole-4-carboxylic acid **2** (190mg, 0.76) were dissolved in a mixture of dry THF (36mL) and NEt_3 (7mL) and the solution was degassed with N_2 for 10min. Then, $Pd_2(dba)_3$ (42mg, 0.046mmol) and $ASPh_3$ (100mg, 0.30mmol) were added to the mixture. The solution was refluxed for 4 hours under N_2. The solvent was removed under reduced pressure. After that, the residue was purified by column chromatography (silica gel) using DCM/CH_3OH =20/1 as eluent. Recrystallization from CH_3OH/Ether to give **LCVC01** (180mg, 74%) ^{1}H NMR (THFd-8, 400 MHZ) δ_H: 9.97 (d, J=4.6Hz, 2H); 9.04 (d, J=4.6Hz, 2H); 8.81 (d, J=4.6Hz, 2H); 8.55 (d, J=4.6Hz, 2H); 8.54 (s, 1H); 8.30 (d, J=7.6Hz, 1H); 7.67 (t, J=8.4Hz, 2H); 7.20 (d, J=8.4Hz, 4H); 7.04 (d, J=8.4Hz, 4H); 6.92 (d, J=8.4Hz, 4H); 3.87 (t, J=6.3Hz, 8H); 2.47 (t, J=7.4Hz, 4H); 1.58-1.51 (m, 4H); 1.36-1.27 (m, 12H); 1.00-0.57 (m, 66H).

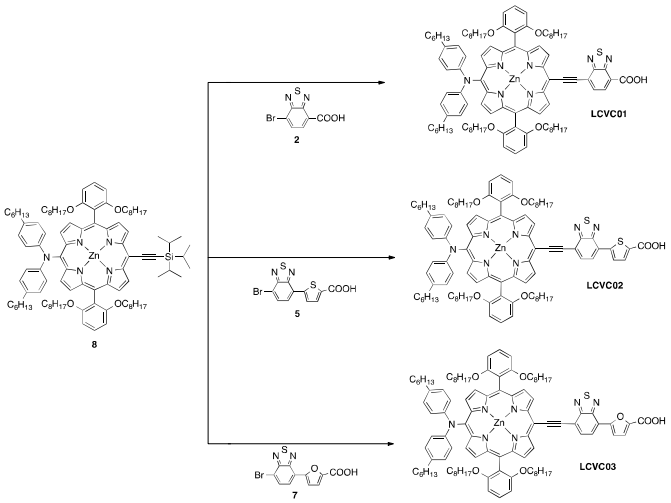

Scheme 2: Synthetic route for the LCVC01, LCVC02 and LCVC03 dyes. (Reaction conditions: (i) TBAF 1M in THF, THF, 30 minutes, 23ºC, 2, NEt_3, $Pd_2(dba)_3$, $ASPh_3$, THF, 4 h, reflux; (ii) TBAF 1M in THF, THF, 30 minutes, 23ºC, 5, NEt3, $Pd_2(dba)_3$, $ASPh_3$, THF, 4 h, reflux; (iii) TBAF 1M in THF, THF, 30 minutes, 23°C, 7, NEt_3, $Pd_2(dba)_3$, $ASPh_3$, THF, 4 h, reflux).

Synthesis of LCVC02: To a solution of [5-Bis(4-hexylphenyl)amino-15-(Triisopropylsily)ethynyl-10,20-bis(2,6-di-octooxyphenyl)porphirinato] Zinc(II) **8** (165mg, 0.106mmol) in dry THF (15mL) was added TBAF (0.54mL) 1M in THF. The solution was stirred at 23ºC for 30min under N_2. The mixture was quenched with H_2O and then extracted with CH_2Cl_2. The organic layer was dried anhydrous $MgSO_4$ and the solvent was removed under reduced pressure. The residue and 5-(7-bromobenzo[*c*][1,2,5]thiadiazol-4-yl)thiophene-2-carboxylic acid **5** (180mg, 0.53mmol) were dissolved in a mixture of dry THF (30mL) and NEt_3 (4.8mL) and the solution was degassed with dinitrogen for 10min. Then, $Pd_2(dba)_3$

(29mg, 0.031mmol) and $ASPh_3$ (71mg, 0.212mmol) were added to the mixture. The solution was refluxed for 4 hours under N_2. The solvent was removed under reduced pressure. Then, the residue was purified by column chromatography (silica gel) using DCM/CH_3OH =20/1 as eluent. Recrystallization from CH_3OH/Ether to give **LCVC02** (115mg, 66%) ^{1}H NMR (THFd-8, 400 MHZ) δ_H: 9.96 (d, J=4.6Hz, 2H); 9.03 (d, J=4.6Hz, 2H); 8.80 (d, J=4.6Hz, 2H); 8.55 (d, J=4.6Hz, 2H); 8.27 (s, 2H); 8.24 (d, J=4.0Hz, 1H); 7.84 (d, J=4.0Hz, 1H); 7.65 (t, J=8.4Hz, 2H); 7.19 (d, J=8.4Hz, 4H); 7.02 (d, J=8.4Hz, 4H); 6.91 (d, J=8.0Hz, 4H); 3.85 (t, J=6.4Hz, 8H); 2.46 (t, J=7.3Hz, 4H); 1.59-1.51 (m, 4H); 1.28 (m, 12H); 0.97-0.55 (m, 66H). ^{13}C NMR (100MHz, THF-d8, ppm) δ□160.78; 156.76; 153.02; 152.11; 151.53; 151.28; 151.02; 134.90; 132.57; 132.06; 131.27; 130.81; 130.42; 130.34; 129.16; 128.21; 127.29; 122.39; 121.49; 121.46; 115.27; 105.71; □□□□□□□□□□□□□□□□□□□□.54; 32.36; 30.45; 29.58; 29.50; 29.40; 25.98; 23.32; 23.10; 14.23; 14.10 MS-ESI (*m/z*): $[M+Na]^+$ calculated for $C_{101}H_{121}N_7NaO_6S_2Zn$: 1678.8003; found: 1678.7963. (^{1}H-NMR/^{13}C-NMR and HRMS(ESI) spectra are shown in the supporting Information)

Synthesis of LCVC03: To a solution of [5-Bis(4-hexylphenyl)amino-15-(Triisopropylsily)ethynyl-10,20-bis(2,6-di-octooxyphenyl)porphirinato] Zinc(II) **8** (150mg, 0.09mmol) in dry THF (15mL) was added TBAF (0.50mL) 1M in THF. The solution was stirred at 23ºC for 30min under N_2. The mixture was quenched with H_2O and then extracted with CH_2Cl_2. The organic layer was dried anhydrous $MgSO_4$ and the solvent was removed under reduced pressure. The residue and 5-(7-bromobenzo[*c*][1,2,5]thiadiazol-4-yl)furan-2-carboxylic acid **7** (146mg, 0.45) were dissolved in a mixture of dry THF (24mL) and NEt_3 (4mL) and the solution was degassed with N_2 for 10min. Then, $Pd_2(dba)_3$ (24mg, 0.026mmol) and $ASPh_3$ (60mg, 0.18mmol) were added to the mixture. The solution was refluxed for 4 hours under N_2. The solvent was removed under reduced pressure. The residue was purified by column chromatography (silica gel) using DCM/CH_3OH =20/1 as eluent. Recrystallization from CH_3OH/Ether to give **LCVC03** (112mg, 76%). ^{1}H NMR (THFd-8, 400 MHZ) δ_H: 9.80 (d, J=4.6Hz, 2H); 8.87 (d, J=4.6Hz, 2H); 8.63 (d, J=4.6Hz, 2H); 8.38 (d, J=4.6Hz, 2H); 8.20 (dd, J=7.7Hz, 21.0Hz 2H); 7.76 (d, J=3.6Hz, 1H); 7.49 (t, J=8.3Hz, 2H); 7.24 (d, J=3.6Hz, 1H); 7.03 (d, J=8.7Hz, 4H); 6.86 (d, J=8.7Hz, 4H); 6.75 (d, J=8.7Hz, 4H); 3.70 (t, J=6.5Hz, 8H); 2.29 (t, J=7.4Hz, 4H); 1.40-1.31 (m, 4H); 1.12 (m, 12H); 0.82-0.46 (m, 66H). ^{13}C NMR (100MHz, THF-d8, ppm) δ□160.78; 156.75; 153.03; 152.10; 151.88; 151.53; 151.28; 151.02; 134.90; 132.58; 132.05; 131.32; 130.82; 130.34; 129.16; 125.75; 123.94; 122.40; 121.49; 115.27; 114.39; 105.17□□□□□□□□□□□□□□□□□□□□ 32.54; 32.36; 29.91; 29.60; 29.50; 29.40; 25.98; 23.32; 23.10; 14.23; 14.10 MS-ESI (*m/z*): $[M]^+$ calculated for $C_{101}H_{121}N_7O_7SZn$: 1639.8334; found: 1639.8365. (^{1}H-NMR/^{13}C-NMR and HRMS(ESI) spectra are shown in the supporting Information).

Solar cell preparation.

The working and counter electrodes consisted of mesoporous TiO_2 and thermalized platinum films, respectively, deposited onto F-doped tin oxide (FTO, Pilkington Glass Inc. with 15 Ω sq^{-1} sheet resistance) conducting glass substrates. Two different types of TiO_2 films were utilized depending on the measurements being conducted. In one hand, highly transparent thin films (8 μm thick) were utilized for L-TAS measurements. On the other hand, efficient DSC devices were made using 14 μm thick films consisting of 20 nm TiO_2 nanoparticles (Dyesol© paste) and a scatter layer of 4 μm of 400 nm TiO_2 particles (CCIC, HPW-400). Prior to the deposition of the TiO_2 paste the conducting glass substrates were immersed in a solution of $TiCl_4$ (40 mM) for 30 minutes and then dried. The TiO_2 nanoparticle paste was deposited onto a conducting glass substrate using the screen printing technique. The TiO_2 electrodes were gradually heated under an airflow at 325 ºC for 5 min, 375 ºC for 5 min, 450 ºC for 15 min and 500 ºC for 15 min. The heated TiO_2 electrodes were immersed again in a solution of $TiCl_4$ (40 mM) at 70 ºC for 30 min and then washed with ethanol. The electrodes were heated again at 500 ºC for 30 min and cooled before dye adsorption. The active area for devices was 0.16 cm^2. The counter electrode was made by spreading a 5 mM solution of H_2PtCl_6 in isopropyl alcohol onto a conducting glass substrate a small hole to allow the introduction of the liquid electrolyte using vacuum, followed by heating at 400ºC for 15 minutes. All films were sensitized in dye solutions at concentrations of 0.125 mM in ethanol containing an excess of chenoxydecholic acid were prepared and the film immersed overnight at room temperature. The sensitized electrodes were washed with ethanol and dried under air. Finally, the working and counter electrodes were sandwiched together using a thin thermoplastic (Surlyn©) frame that melts at 100 ºC. The electrolytes used consisted of 0.5 M 1-butyl-3-methylimidazolium iodide (BMII), 0.1 M lithium iodide, 0.05 M iodine and 0.5 M *tert*-butylpyridine in acetonitrile.

Device characterization

The IV characteristics of cells were measured using a Sun 2000 Solar Simulator (150 W, ABET Technologies). The illumination intensity was measured to be 100 mW/m^2 with a calibrated silicon photodiode. The appropriate filters were utilized to faithfully simulate the AM 1.5G spectrum. The applied potential and cell current were measured with a Keithley 2400 digital source meter. The IPCE (Incident Photon to Current conversion Efficiency) was measured using a home made set up consisting of a 150 W Oriel Xenon lamp, a motorized monochromator and a Keithley 2400 digital source meter.

Transient photovoltage (TPV) and charge extraction (CE) measurements were carried out on a system are reported before by our own group[7a]. In the CE measurements, white light from a series of LEDs was used as the light source. When the LEDs are turned off the cell is immediately short circuited and the charge is extracted allowing electron density in the cells to be calculated. By changing the LEDs intensity the electron density

can be estimated as a function of cell voltage. In TPV measurements in addition to the White light applied by the LEDS, constant background voltage is applied to the cells and again, a diode pulse (660 nm, 10 mW) is then applied to the sample inducing a change of 2-3 mV within the cell voltage. The resulting photovoltage decay transients are collected and the τ values are determined by fitting the data to a first order decay (equation $\exp(-t/\tau)$).

Laser-transient absorption spectroscopy (L-TAS) measurements were similar to those carried out previously[7b]. The kinetics were recorded in a blank electrolyte consisting of 0.5M *tert*-butylpyridine in acetonitrile and the iodide/tri-iodide electrolyte used for the optimized 0.16cm^2 devices.

2.4 Theoretical calculations

The molecules were optimized with Gaussian09 code[8]. The functional of choice was B3LYP[9] and the basis set was 6-31g(d)[10]. The frontier molecular orbitals were plot at the same density.

3. Results and discussion

In Figure 3 we can see the UV-Visible absorption spectra for the **LCVC01**, **LCVC02** and **LCVC03 dyes.** Their photophysical and electrochemical characteristics are listed in Table 1.

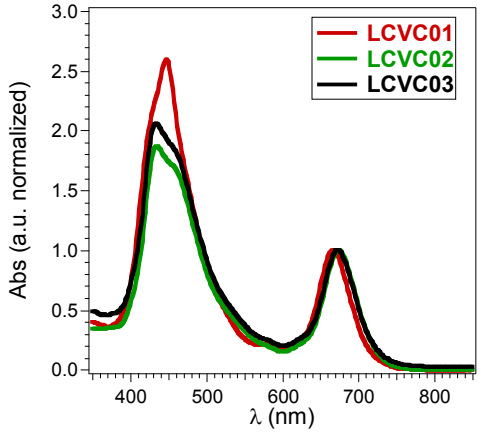

Figure 3: UV-Visible absorption spectra of **LCVC01**, **LCVC02** and **LCVC03** in THF

As shown in Figure 3 all the dyes exhibit typical porphyrin spectra with the bands associated to them. Centred at λ= 450nm we observe an intense Soret band and between 600-700nm a less intense Q-band.

Table 1. Absorption, emission and electrochemical properties of **LCVC01, LCVC02** and **LCVC03**

Dye	λ_{abs} (nm)[a]	λ_{em} (nm)[a]	E_{ox} (V v's Fc/Fc+)[b]	$E_{0\text{-}0}$ (eV)[c]	E_{HOMO} (eV)[d]	E_{LUMO} (eV)[e]
LCVC 01	448; 579; 668	705	0.19	1.82	-5.07	-3.25
LCVC 02	434; 674	715	0.17	1.81	-5.05	-3.24
LCVC 03	434; 674	690	0.17	1.82	-5.05	-3.23

[a]Measured in Tetrahidrofuran. In parenthesis molar extinction efficient at λ_{abs} (in M^{-1} cm^{-1}). [c]$E_{0\text{-}0}$ was determined from the intersection of absorption and emission spectra in dilute solutions. [d]E_{HOMO} was calculated using E_{HOMO}(vs vacuum) = -4.88-E_{ox}(vs Fc/Fc+). [e]E_{LUMO} was calculated using $E_{LUMO} = E_{HOMO} + E_{0\text{-}0}$.

The oxidation potentials of porphyrins were measured by cyclic voltammetry. (see SI Fig:13) in THF. **LCVC02** and **LCVC03** present the same oxidation potential. However, the potential is 20mV lower when compared to **LCVC01**. This is due to the presence of the thiophene and the furan moieties, between the BDT group and the carboxylic acid in **LCVC02** and **LCVC03** respectively.

We do not observe a great difference in the HOMO and LUMO energy levels between the molecules. The HOMO energy value ensures efficient dye regeneration by the electrolyte and the LUMO energy value is high enough to make possible efficient electron transfer from the dye excited state into the TiO_2 conduction band (E_{TiO2}= -4.0 eV).

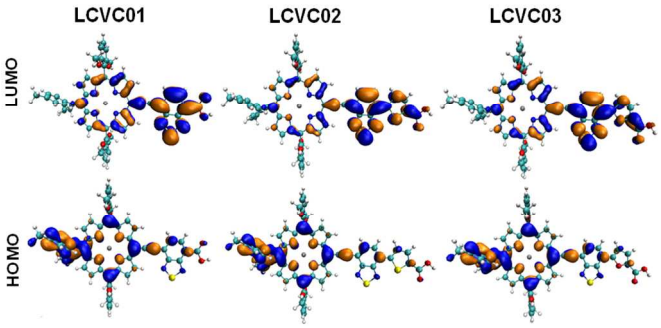

Figure 4: Frontier molecular orbitals of **LCVC01**, **LCVC02** and **LCVC03** at the B3LYP/6-31G (d) level

Comparing the theoretical frontier orbitals between the three molecules we observed that the probability to find the highest occupied molecular orbital (HOMO) of three dyes is located predominantly on the donor moiety of the molecule. The probability to localize the lowest unoccupied molecular orbital (LUMO) is similar for **LCVC02** and **LCVC03** showing a significant shift through the acceptor due to the presence of the BDT acting as an electron drawing moiety that we do not observe the for the **LCVC01** dye. Tacking into account this observation we can explain the higher charge transfer character for the **LCVC02** and **LCVC03** porphyrins. The main difference between **LCVC02** and **LCVC03** is the larger contribution of the 3p orbital of S in **LCVC02** to the LUMO.

In addition the dyes present different dipolar moments, Table 2. For **LCVC01** a large dipole value aligned parallel (μ_x) to the carboxylate anchoring group can induce a severe band-shift (upwards) when adsorbed on the surface, thus hindering charnge injection. **LCVC03** presents a large component out of the plane of the porphyrin ring (μ_z) that inducs dipole-dipole interactions in the dye layer. **LCVC02**

presents thus a compromise minimizing the dipole contributions that can compromise injection.

Table 2. Dipole moment of the dye molecules Cartesian components and module

Porphyrin	μ_x(D)	μ_y(D)	μ_z(D)	$\|\mu\|$(D)
LCVC01	5.15	-0.48	-0.05	5.17
LCVC02	4.68	2.95	-0.27	5.54
LCVC03	3.00	3.06	-1.00	4.40

The **LCVC01**, **LCVC02** and **LCVC03** were used to fabricate DSSC solar cells and measured under illumination conditions (AM 1.5G 100 mW/m^2). The device properties are listed in Table 3.

Table 3. Solar cell parameter for our best-measured devices.

Porphyrin	Voc (V)	Jsc (mA/cm^2)	FF (%)	Efficiency (%)*
LCVC01	0.65	7.69	75	3.84 (4.52)
LCVC02	0.70	20.00	74	10.41 (12.1)
LCVC03	0.58	5.81	76	2.55 (2.88)

*Efficiencies recorded with mask. In parenthesis the efficiency values without mask.

The photocurrent density observed for **LCVC01** and **LCVC03** is lower when compared to **LCVC02.** The best J_{sc} corresponds to **LCVC02** that displays an impressive 20.00 mA/cm^2, such current is actually as high as most MAPI solar cells, in contrast with the 7.7 and 5.8 achieved for **LCVC01** and **LCVC03** respectively. The photocurrent matches the calculated photocurrent after integration of the IPCE spectrum (Figure 5b) against the 1.5 AM G solar spectrum provided by NREL lab (Excel file at the SI) with a 5% error due to the mismatch factor of our solar simulator. The open circuit voltage (V_{oc}) for **LCVC01** is 650mV. As reported before the introduction of a spacer group between the BDT and the anchoring group, as in the case of **LCVC02**, leads to a substantial increase in V_{oc}. However, in our case, this effect is not observed for **LCVC03** with a V_{oc} as low as 580mV. Yet, all solar cells present similar values for the fill-factor (FF).

In Figure 5a we represented the I-V curves for **LCVC01**, **LCVC02** and **LCVC03**. Figure 5b illustrates the incident-photon-to-current conversion efficiency (IPCE) of our champion cell made using porphyrin **LCVC02**. The IPCE spectrum values showed two maxima corresponding to the Soret and Q bands of the porphyrin at 480nm (76%) and 670nm (90%).

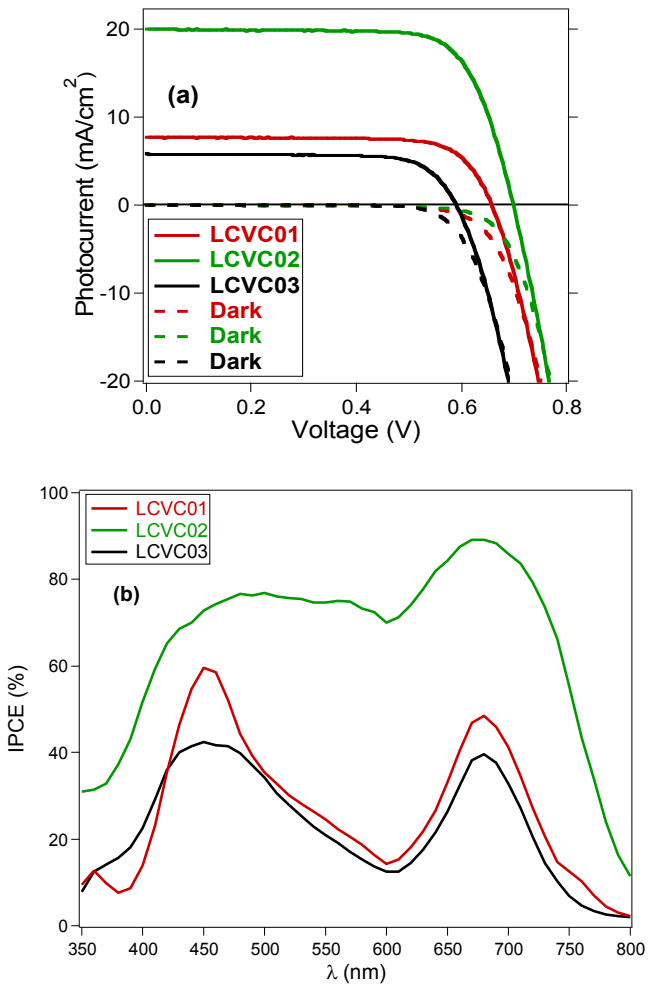

Figure 5. (a) I-V curves for **LCVC01, LCVC02** and **LCVC03** (b) IPCE spectra of **LCVC02.** DSSC devices recorded under AM 1.5G radiation. The dashed lines correspond to the IV dark curves.

The electron density (defined as the number of electrons accumulated at the m-TiO_2) and the electron lifetime (Figure 6a and 6b) were probed using charge extraction and transient photovoltage measurements respectively. We observed higher charge (electron) density for **LCVC02** when compared to **LCVC01**. However the larger difference is observed when we compare to **LCVC03** that presents a much lower charge density. Moreover, a clear shift of the exponential curve from, 0.5 to 0.6V can be seen for **LCV03**. This shift can be correlated with a shift of the TiO_2 conduction band edge that leads to a decrease in the photo-injection yield of electrons from the dye-excited state, and therefore the device phototocurrent. The TiO_2 conduction band shift has been previously reported to occur by changes at the surface of the TiO_2 due to different dipoles, protonation or addition of, for example tert-butyl pyridine at the liquid electrolyte as additive to enhance the device V_{oc} by at expenses of device photocurrent. In our case, is probably due to the large μ_x component of the dye. From the TPV measurements (Figure 6b), slower recombination dynamics can be seen for **LCVC02** and a similar electron lifetime is also observed for **LCVC01**, which explains the similar voltage achieved for these devices, which is in agreement with the shortest electron lifetime for **LCVC03** too. The differences

obtained can be explained due to the differences in the e-TiO_2/electrolyte$^+$ recombination rate. Several studies reported before by our group and others show that this experimental observation is true for organic sensitizers[11] and ruthenium complexes[12]. Due to this, more species, I_2 according to O'Regan and co-workers[13], are present at the TiO_2 surface accelerating the recombination rate. In our present study, we have seen how this hypothesis effects a change in the device performance by just the change of only one atom in the molecular structure.

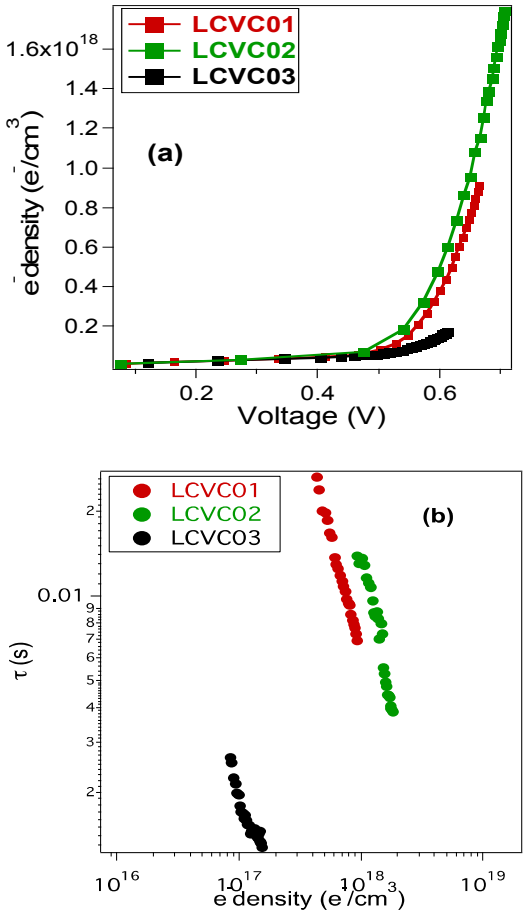

Figure 6. (a) Electron density as a function of cell voltage and (b) Electron density as a function of cell voltage for **LCVC01, LCVC02** and **LCVC03** devices.

Yet, we must also demonstrate that differences observed between the porphyrins are not due to differences in the regeneration kinetics. In order to probe dye ground state regeneration by the I_3^-/I^- redox couple we employed laser transient absorption spectroscopy (L-TAS).

In Figure 7 we can see the charge recombination decays between the photo-injected electrons at the TiO_2 and the oxidized dye for **LCVC01**, **LCVC02** and **LCVC03** respectively. The data was recorded in absence of electrolyte (black) and corresponds to the long-lived decays assigned to the dye cation formed following photo-excitation. In red color we monitored the same process but in the presence of electrolyte. As can be seen the kinetics for the dye cation disappearance is much faster due to the regeneration by I^-. To estimate the regeneration efficiency we quantified the lifetime at the FWHM (full with at half maximum) of the signal, in red, which is within the same millisecond time scale for all three different solar cells for **LCVC01**, **LCVC02** and **LCVC03** showing marginal differences which cannot account for the large differences observed for the devices under sun-simulated standard illumination conditions

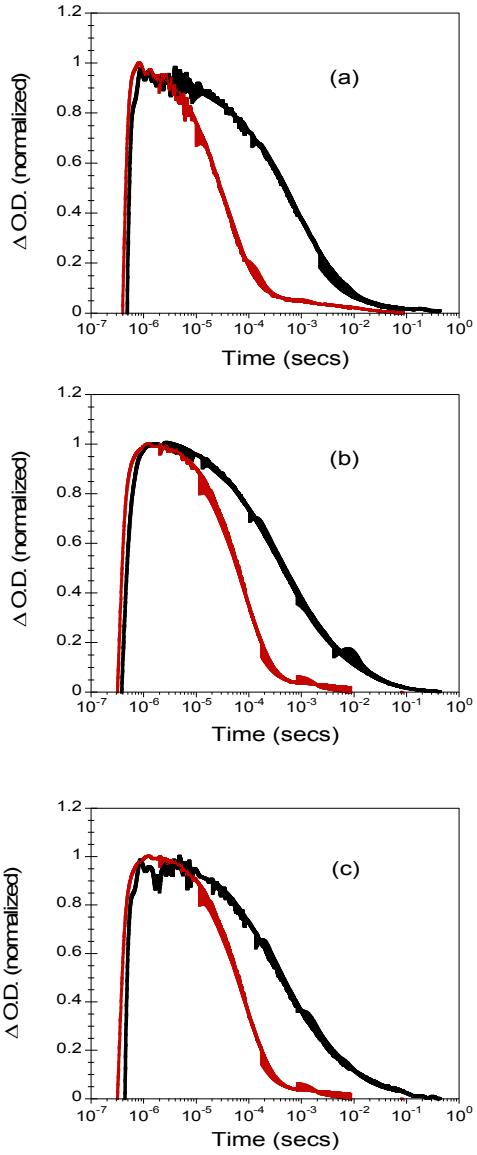

Figure 4. Transient absorption kinetics of (a) **LCVC01**, (b) **LCVC02** and (c) **LCVC03** recorded for 1cm^2 area devices comprising 8 µm TiO_2 films in the presence of a blank electrolyte (black) and an iodide/tri-iodide red/ox electrolyte (red). Kinetics were recorded at 825nm for LCVC01, 775nm forLCVC02 and 825nm for LCVC03 following excitation at 600nm.

4. Conclusions

We have been synthesized a new series of push pull porphyrins using a diphenylamine as a donor moiety and an acid group as anchoring group with the introduction of a BDT group between the porphyrin core and the anchoring group for **LCVC01** and the introduction of a thiophene and a furan between the BDT and the anchoring group for **LCVC02** and **LCVC03** dyes. The DSSC performance gave us a record cell of 10.4% for **LCVC02**, however only a 3.84% and 2.55% were achieved for **LCVC01** and **LCVC03** respectively. As we have studied in the past the thiophene introduced in **LCVC02** reduces the

recombination reaction. However, the introduction of a furan moiety does not make the same effect. In that case, the major effect is the decrease in photocurrent. Moreover, from the charge extraction measurements a clear change of the TiO_2 conduction band edge can be registered that can be the consequence of a change of the dye dipole at the surface leading to lower electron injection yield in good agreement with the lower measured photocurrent. Therefore, in dye design dipole descriptors shall be incorporated. Further work is been explored in this direction.

Acknowledgements

EP would like to thank MINECO for the project CTQ2013-47183-R and the support through Severo Ochoa Excellence Accreditation 2014-2018 (SEV-2013-0319).

Notes and references

[a] Institute of Chemical Research of Catalonia (ICIQ). Avda. Països Catalans, 16. Tarragona. E-43007. Spain.

[b] Catalan Institution for Research and Advanced Studies (ICREA). Passeig Lluís Companys, 23. Barcelona E-08010. Spain.

† It is known that MAPI solar cells have different efficiencies depending on the voltage scan rate and direction being most favourable the "reverse direction" meaning from open-circuit voltage to short-circuit photocurrent.

†† http://www.forumforthefuture.org/greenfutures/articles/massive-solar-façade-swiss-convention-centreupplementary

Information (ESI) available: The ^{1}H-NM, ^{13}C-NMR, HRMS (High Resolution Mass Spectra) and Cyclic Voltammetry for the porphyrins. See DOI: 10.1039/b000000x/

References.

1 S. Mathew, A. Yella, P. Gao, R. Humphry-Baker, F. E. CurchodBasile, N. Ashari-Astani, I. Tavernelli, U. Rothlisberger, K. Nazeeruddin, Md. and M. Grätzel, *Nat. Chem.*, 2014, **6**, 242-247.

2 H. J. Snaith, *Adv. Funct. Mat.*, 2010, **20**, 13-19.

3 T. Bessho, S. M. Zakeeruddin, C.-Y. Yeh, E. W.-G. Diau and M. Grätzel, *Angew. Chem. Int. Ed.*, 2010, **49**, 6646-6649.

4 A. Yella, H.-W. Lee, H. N. Tsao, C. Yi, A. K. Chandiran, M. K. Nazeeruddin, E. W.-G. Diau, C.-Y. Yeh, S. M. Zakeeruddin and M. Grätzel, *Science*, 2011, **334**, 629-634.

5(a) Y.-C. Chang, C.-L. Wang, T.-Y. Pan, S.-H. Hong, C.-M. Lan, H.-H. Kuo, C.-F. Lo, H.-Y. Hsu, C.-Y. Lin and E. W.-G. Diau, *Chem. Comm.*, 2011, **47**, 8910-8912; (b) C.-H. Wu, M.-C. Chen, P.-C. Su, H.-H. Kuo, C.-L. Wang, C.-Y. Lu, C.-H. Tsai, C.-C. Wu and C.-Y. Lin, *J. Mat. Chem. A*, 2014, **2**, 991-999; (c) Y. Wang, B. Chen, W. Wu, X. Li, W. Zhu, H. Tian and Y. Xie, *Angew. Chem. Int. Ed.*, 2014, **53**, 10779-10783; (d) L. Pelleja, C. V. Kumar, J. N. Clifford and E. Palomares, *J. Phys. Chem. C*, 2014, **118**, 16504-16509; (e) M. Tanaka, S. Hayashi, S. Eu, T. Umeyama, Y. Matano and H. Imahori, *Chem. Commun.*, 2007, 2069-2071.

6(a) L. Zhao, P. Wagner, A. B. S. Elliott, M. J. Griffith, T. M. Clarke, K. C. Gordon, S. Mori and A. J. Mozer, *J. Mat. Chem. A*, 2014, **2**, 16963-16977; (b) M. J. Griffith, K. Sunahara, P. Wagner, K. Wagner, G. G. Wallace, D. L. Officer, A. Furube, R. Katoh, S. Mori and A. J. Mozer, *Chem. Commun.*, 2012, **48**, 4145-4162.

7(a) D. Joly, L. Pellej√†, S. Narbey, F. Oswald, J. Chiron, J. N. Clifford, E. Palomares and R. Demadrille, *Sci. rep.*, 2014, **4**; (b) J. Clifford, A. Forneli, L. Lopez-Arroyo, R. Caballero, P. de la Cruz, F. Langa and E. Palomares, *ChemSusCHem*, 2009, **2**, 344-349.

8 M. J. Frisch. et al., *Gaussian 09 Revision D.01*, Gaussian. Inc. Wallingfrod CT, 2009.

9 P. J. Stephens, F. J. Devlin, C. F. Chabalowski and M. J. Frisch, *J. Phys. Chem.*, 1994, **98**, 11623-11627.

10 V. A. Vassolov, J. A. Pople, M. A. Ratner and T. L. Windus, *J. Chem. Phys.*, 1998, **109**, 1223-1229.

11(a) M. Planells, L. Pelleja, J. N. Clifford, M. Pastore, F. De Angelis, N. Lopez, S. R. Marder and E. Palomares, *Energ. Envir. Sci.*, 2011, **4**, 1820-1829; (b) J.-I. Nishida, T. Masuko, Y. Cui, K. Hara, H. Shibuya, M. Ihara, T. Hosoyama, R. Goto, S. Mori and Y. Yamashita, *J. Phys. Chem. C*, 2010, **114**, 17920-17925; (c) B. C. O'Regan, I. Lopez-Duarte, M. V. Martinez-Diaz, A. Forneli, J. Albero, A. Morandeira, E. Palomares, T. Torres and J. R. Durrant, *J. Am. Chem. Soc.*, 2008, **130**, 2906-2907.

12(a) K. Hu, H. A. Severin, B. D. Koivisto, K. C. D. Robson, E. Schott, R. Arratia-Perez, G. J. Meyer and C. P. Berlinguette, *J. Phys. Chem. C*, 2014, **118**, 17079-17089; (b) A. Reynal, A. Forneli, E. Martinez-Ferrero, A. Sanchez-Diaz, A. Vidal-Ferran, B. O'Regan and E. Palomares, *J. Am. Chem. Soc.*, 2008, **130**, 13558-13567.

13 C. E. Richards, A. Y. Anderson, S. Martiniani, C. Law and B. C. O'Regan, *J. Phys. Chem. Lett.*, 2012, **3**, 1980-1984.

